

## RESEARCH ARTICLE

# Biosynthesis of Silver Nanoparticles using *Annona squamosa* L Seed and Leaves Extract: Evaluation of the Anti-inflammatory, Antifungal, and Antibacterial Potency

Yogesh Kolekar<sup>1</sup>, Firoj Tamboli<sup>1\*</sup>, Dinanath Gaikwad<sup>2</sup>, Shabana Memon<sup>3</sup>, Sampada Gulavani<sup>3</sup>, Kamal Alaskar<sup>3</sup>, Dipak Mali<sup>4</sup>, Vijaykumar Pawar<sup>5</sup>

<sup>1</sup>Department of Pharmacognosy, Bharati Vidyapeeth College of Pharmacy, Kolhapur, Maharashtra, India.

<sup>2</sup>Department of Pharmaceutics, Bharati Vidyapeeth College of Pharmacy, Kolhapur, Maharashtra, India

<sup>3</sup>Bharati Vidyapeeth (Deemed to be University)'s Institute of Management, Kolhapur, Maharashtra, India.

<sup>4</sup>Department of Quality Assurance, Krishna Institute of Pharmacy, Krishna (Deemed to be University), Karad, Maharashtra, India.

<sup>5</sup>Department of Pharmaceutical Chemistry, Bharati Vidyapeeth College of Pharmacy, Kolhapur Maharashtra, India

Received: 10<sup>th</sup> January, 2023; Revised: 04<sup>th</sup> March, 2023; Accepted: 13<sup>th</sup> May, 2023; Available Online: 25<sup>th</sup> June, 2023

## ABSTRACT

Creating efficient therapeutic techniques against multi-drug resistant pathogens is crucial in the age of rising bacterial resistance and infectious disease outbreaks. In this case, *Annona squamosa* seed and leaf extract were used to create silver nanoparticles, which were then assessed using various characterization techniques, including UV-vis scanning electron microscopy, X-ray powder diffraction, particle size, and Fourier-transform infrared spectroscopy. The synthesized AgNPs were tested for their ability to combat a variety of gram-positive and gram-negative bacteria as well as their ability to control free radicals and inflammation brought on by skin damage caused by microbial infection. AgNPs from seeds have a greater effect than those from leaves, so they were used to create several batches of gel formulation utilizing different gelling agents such as HPMC, chitosan, and Carbopol. Gel was also evaluated for its physical characteristics, including color, clarity, pH, viscosity, spreadability, and extrudability. It also underwent a centrifugation test and a drug release test. Since the F6 batch outperformed the other batches in the evaluation test, it was chosen to evaluate the antibacterial and antifungal activity.

**Keywords:** Silver nanoparticles, Antimicrobial, Antioxidant, Anti-inflammatory.

International Journal of Pharmaceutical Quality Assurance (2023); DOI: 10.25258/ijpqa.14.2.23

**How to cite this article:** Kolekar Y, Tamboli F, Dinanath Gaikwad D, Memon S, Gulavani S, Alaskar K, Mali D, Pawar VK. Biosynthesis of Silver Nanoparticles using *Annona squamosa* L Seed and Leaves Extract: Evaluation of the Anti-inflammatory, Antifungal, and Antibacterial Potency. International Journal of Pharmaceutical Quality Assurance. 2023;14(2):377-387.

**Source of support:** Nil.

**Conflict of interest:** None

## INTRODUCTION

Taniguchi coined the phrase “nanotechnology” for the first time in 1974. He claims that the merging, distortion, and parting of materials by a single fragment or atom are the processes of nanotechnology.<sup>1</sup> Nanotechnology aims to monitor and manage matter at the nanoscale; its dimension ranges from 1 to 100 nm.<sup>2</sup> Nanoparticles are regarded as a component of nanotechnologies that use natural resources and are successfully applied in the field of biological and medical research. Nanoparticles are incredibly potent and crucial building blocks for new research bases because of their unique features.<sup>3</sup> It is well recognized that green technologies have more advantages once equated to traditional chemical or physical progressions for producing nanoparticles. A crucial benefit of this technology is that it has

a minimal negative environmental impact because it follows the principles of green chemistry and is also more efficient and affordable. And yet another benefit is that scaling up the process to an industrial level is simple.<sup>4-6</sup>

Due to the abundance of phytochemicals, plants serve as the primary medium for the synthesis and development of nanoparticles.<sup>7</sup> Nanoparticles were used in a variety of ways in the separate industries of pharmaceuticals, electronics, medicine, and diagnostic tools. Silver nano-molecules have a comprehensive assortment of medical uses, including treatment such as burn victims, antibacterial activity, targeted medication delivery, and more.<sup>8</sup> Fighting microbes aids in encompassing the serviceable life of food. The biological method of creating silver nanoparticles is both economical and

\*Author for Correspondence: drfatamboli@gmail.com

environmentally benign. Additionally, the simplest technique to create nanoparticles is by biosynthesis.<sup>9,10</sup>

Fruit trees like *A. squamosa* L. (*ACEAE*) have a long history of traditional applications. An evergreen plant called *A. squamosa* can be found primarily in tropical and subtropical climates. *A. squamosa* is frequently used to make drinks, ice cream, and candies. Different parts of *A. squamosa* have been linked to a variety of ethno-medical purposes, including tonic, apophlegmatisant, aborticide, and cardiac tranquilizing.<sup>11</sup> Utilizing food waste nowadays is crucial to reducing waste production and waste-related issues. That is why custard apple trash, which is gathered after pulp removal, is employed in the biosynthetic process.<sup>12</sup> Compared to traditional chemical or physical techniques of nanoparticle production, the amalgamation of Ag-NP consuming a leftover part of the plant-material (i.e., seed & leaves) provides economic and environmental advantages.<sup>13-15</sup>

### Mechanism of Action of Silver Nanoparticles

Although the literature has revealed that these particles can interact with bacterial membranes,<sup>16</sup> the precise mechanism behind the antibacterial actions of AgNPs is yet unknown. AgNPs may interact with bacteria and produce reactive oxygen species and free radicals, which damage intracellular organelles and alter intracellular signaling pathways that lead to apoptosis.<sup>17,18</sup> This is one such hypothesized mechanism. AgNP adherence to the bacterial wall, followed by the particles' penetration and bacterial cell membrane disruption that causes the release of cellular contents and death, is another widely recognized mechanism of bacterial cytotoxicity.<sup>19-24</sup>

## MATERIALS AND METHODS

### Plant Material

The plant material for the proposed study was collected and confirmed by Prof. D.G. Jagtap Head, Dept. of Botany, Shri. Vijaysinha Yadav College Peth Vadgaon, Kolhapur.

### Methods

#### Preparation of extract

Seeds and leaves were washed several times with tap water and then finally with double distilled water to remove dust particles and unwanted foreign particles. Seeds were dried in oven at 60°C for 6 hours; leaves were dried in shade for 7 days separately. Then seed and leaves were crushed using a mixer and powdered material kept it in a glass container for next use. The extract of seed and leaves were prepared with use of as aqueous extracts. Around 20 gm of powder was added in 200 mL of H<sub>2</sub>O and heated at 70 to 80°C for 30 minutes. Cool and filter it and centrifuge at 2000 rpm. Afterward, phytochemical screening of the prepared extract was carried out.

#### Synthesis of silver NP's

Synthesis of the silver NPMs with use of aq. extract of *A. squamosa* L. seeds and leaves:

Make 0.01M liquid of silver nitrate 50 mL in 250 mL conical flask, assorted with 10 mL of freshly prepared extract

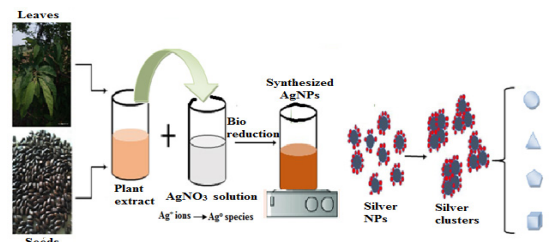


**Figure 1:** Synthesis of AgNPs of *A. squamosa* L. leaves and seeds through green synthesis

of aqueous *A. squamosa* L. seed and leaves separately. Stir the above combination with a magnetic stirrer at 50°C for 15 to 20 minutes. Centrifuge the solution and gather the pellets. Afterward, dry the residue of silver nanoparticles, collect and store at 4°C in the refrigerator (Figure 1).

### Characterization of Developed Nanoparticles

#### UV-visible spectroscopy

To observe the full bioreduction of AgNO<sub>3</sub> to silver nanoparticles the spectra of the sample or medicament were checked using a Shimadzu U.V. probe1800 in the scanning series 300 to 800 nm with a resolution of 1-nm.

#### SEM

Scanning electron microscopies allow for the direct visual assessment of morphology. These techniques have a wide range of morphological and analysis size advancements and are reliant on electron microscopy, so they can probably only offer limited insight into distribution size.

#### XRD

Any extra particles introduced to X-ray radiation reflected it, resulting in various redirection patterns that reflected the physicochemical characteristics of the crystal structure. The architectural characteristics of a powder illustration or metallic nanoparticle are frequently reflected in diffraction patterns from a specimen.

#### Particle size analyzer

The particle distributions of the size morphology are frequently a key element of their explanations of the NPs. Using imaging techniques the diameters of the morphologies were calculated. Two crucial uses for NPs are the release of pharmaceuticals and the targeting of medications. The drug discharge was found to be the main factor affecting the size of the particles.

#### FTIR

FTIR was skilled with providing accuracy, recall ability, and persistent use when it came to exploring even when macromolecules were used in the production of metallic nanoparticles, which stood out in both their academic and industrial operations. Furthermore, FTIR has been extending to the materials they have been researching at the nanometer scale, along with the verification of bioactive agents covalently grafted onto silver, copper, and zinc together with any other NPs or the interplay among enzymes as well as the subtraction of their catalytic reactions.

## Pharmacological Evaluation of Developed Silver Nanoparticles

### Antibacterial activity

For the best results, the spread plate approach is utilized in conjunction with freshly prepared metallic NP's samples, distilled water, and the antibacterial antibiotic azithromycin (0.3% conc.), which is used as a standard. The antibacterial investigation employs the cultures of *E. coli*, *B. subtilis*, *X. scampetris*, and *S. aureus* is used for the antibacterial study.

### Antifungal activity

For the best results, the spread plate approach is utilized in conjunction with freshly prepared metallic NP samples, distilled water, and the antibacterial medication clotrimazole (0.3% conc.), which serves as a reference. For the antifungal investigation, *A. niger* culture is employed.

### Antioxidant action of established nanoparticles

The inhibition power of the oxidative molecule of prepared AgNPs was checked by spotting the reducing DPPH free radical to their steadiness. Using the stable radical DPPH the free radical rummaging activity of prepared AgNPs of seeds and leaves of plant determined, respectively and compared to normal ascorbic acid. 1-mL of AgNPs at (10, 20, 30, and 40 µg/mL) concentrations were combined with 3.0 mL of newly made DPPH solution separately (1-mM in methanol) and mixed well. After that, the mixture was let to sit at 37°C in the dark for 30 minutes. In order to measure the absorbance, a UV-vis spectrophotometer was used at 517 nm (Shimadzu, UV- 800). Methanol was cast-off as a blank solution and DPPH was cast-off as the control. The DPPH scavenging action was articulated as the fraction of inhibition which was determined using the following formula:

$$\% \text{DPPH Radical Scavenging Activity} = \frac{A_c - A_s}{A_c} \times 100$$

$$IC_{50} = \text{concentration of tested sample} \times 50 / \% \text{ inhibition}$$

## In-vitro Anti-inflammatory Activity

### Inhibition of albumin (protein) denaturation

The scheme outlined below was cast-off to calculate the percentage of protein denaturation inhibition.

#### Controlled approach/solution (50 mL)

A total of 20 mL of distilled water, 14 mL of pH 6.4 phosphate buffer, and 2 mL of egg albumin.

#### Marketed medicine (50 mL)

A total of 2.0 mL of egg albumin, 28 mL of pH-6.4 buffer i.e., phosphate, and 10 mL of standard medication (indomethacin) at 100, 200, 400, 800, and 1000 µg/mL concentrations were used.

#### Test solution (50 mL)

28 mL of phosphate buffer (pH 6.4), 2 mL of egg albumin and 10 mL of various concentrations of prepared AgNPs of *AS* seeds & leaves were prepared in the various concentrations

100.0, 200, 400, 800, and 1000 µg/mL, respectively. A modest amount of 1N HCl was used to correct the pH of each of the above-mentioned solutions. The samples underwent a 15-minute incubation period at 37°C and 5 minute heating period at 70°C. Afterward chilling, the absorbance of the turbid solution was dignified at 660 nm in UV spectrophotometer. Utilizing the following formula, the overhead solutions fraction inhibition of denaturation of protein was computed:

$$\text{Percentage inhibition} = \frac{(\text{Abs. of control} - \text{Abs. of test}) / \text{Abs. of control}}{\times 100}$$

## Preparation of Formulation

While from above data originate AgNPs formulated by utilizing *A. squamosa* L. seeds extract includes enhanced activity than AgNPs prepared by using *A. squamosa* L. leaves extract so we used it for the preparation of formulations. Carbopol, chitosan and HPMC were used as gelling agent in formulations. Gels were formulated by cold mechanical technique (Table 1).

### Carbopolgel

Carbopol was gradually added to the surface of double-distilled water in separately weighed amounts of 1, 1.5, and 2 g, and then mixed for 30 minutes at 1200 rpm on a magnetic mixer. After that, the polymer was given some time to soak in the water. Glycerol was added, and while the gel was continuously agitated, the drug AgNPs dissolved in water was added. After bringing the pH to 6, triethanolamine dropwise added, the blend was gently stirred until a transparent and translucent gel was created.

### Chitosan gel

Chitosan was gradually added to the surface of double-distilled water in separate amounts of 1, 1.5, and 2 g, and then mixed for 30 min. at 1200 rpm on a magnetic mixer. It was added since acetic acid is used in hydrolysis to make it more soluble in water. Glycerol was added, and while the gel was continuously agitated, the drug AgNPs dissolved in water was added. The liquid gently swirled after using triethanolamine to bring the pH to 6. until a transparent, translucent gel was created.

### Hydroxypropyl methylcellulose gel

Weighed individually, 1, 1.5, and 2 g of HPMC were slowly added to the surface of double-distilled water, and then blended for 30 minutes at 1200 rpm on a magnetic mixer. After that, the polymer was given some time to soak in the water. Glycerol was added, and while the gel was continuously agitated, the drug AgNPs dissolved in water was added. The liquid gently swirled after using triethanolamine to bring the pH to 6. until a transparent and translucent gel was created.

## Physicochemical Evaluations

### Estimation of clarity and color

The prepared gel formulations were inspected with the naked eyes for their color and clarity.

**Table 1:** Gel composition with polymers

Ingredients	F1	F2	F3	F4	F5	F6	F7	F8	F9
Carbopol (gm)	1.0	1.50	2.0	-	-	-	-	-	-
Chitosan (gm)	-	-	-	1.0	1.50	2.0	-	-	-
HPMC (gm)	-	-	-	-	-	-	1.0	1.50	2.0
Glycerol (gm)	2.0	2.0	2.0	2.0	2.0	2.0	2.0	2.0	2.0
Silver nano (gm)	0.02	0.02	0.02	0.02	0.02	0.02	0.02	0.02	0.02
Glacial acetic acid (mL)	-	-	-	0.75	1.12	1.5	-	-	-
Tri-ethanolamine	qs								
PW (qs in mL)	100.0	100.0	100.0	100.0	100.0	100.0	100.0	100.0	100.0

#### Estimation of odor

It was done by mixing gel in water and taking the smell.

#### pH

Numerical pH meters were cast-off to measure the pH. of the formulation gels (Make Lab India). In 100 mL of pure water, 1.0 g of gel was dissolved. Each formulation's pH was measured three times, and the average values were calculated.

#### Viscosity

Using spindle number 64 on a Brookfield viscometer (Model RVTDV II) at 100 rpm, the viscosity was found out. The viscometer's corresponding dial reading was recorded. The spindle was then gradually lowered after that. The dial reading should remain consistent as you turn the spindle in the gel.

#### Spreadability

The spreadability value of various gel batches was determined by computing the distribution width of one gram of gel among 2 horizontal glass plates after one minute under a particular force.

#### Extrudability

The gel compositions were placed inside of ordinary collapsible aluminum tubes with caps, and the ends were sealed by crimping them together. Loads of the cylinders were recorded. After being positioned between dual transparent slides, the tubes were tightened. After applying 500 gm on the slides, the cap was removed. The volume of the ejected gel was taken and weighed. Calculated the gel's extrudability percentages (more than 90% outstanding, greater than 80% good, and greater than 70% fair).

#### Centrifugation parameter

For the centrifugation experiment, 10 gm of the formulation were placed in a centrifuge tube. The specimen gel was centrifuged for half an hour. at room temperature, spinning at 2000 rpm.

#### Drug release testing

Franz diffusion cells were used to conduct *in-vitro* diffusion tests on all formulations. As receptor medium, phosphate buffer (pH 7.4) was engaged. Dialysis membranes made of goat film were engaged. The membrane was cut into an appropriate-sized section. Prior to the experiment, goat casing was soaked in phosphate buffer for around 30 minutes. 10 mL of receptor media were put to each cell. On the Franz cells' flat

flange, a membrane was engaged. All cells' ultimate receptor media volume was 12 mL, as indicated on the sampling arm. The cell was shaken to divest yourself of the bubbles. The temperature was maintained using the water circulation jacket. All experiments engaged 50 rpm magnetic stirring. About 6 hours were spent studying. Samples were collected at intervals of 30 minutes, and a UV-vis spectrometer was cast-off to find them at 440 nm. The receptor solution was interchanged with an equivalent volume of brand-new receptor solution following each withdrawal. A release graph was then created by plotting the result against time.

#### Estimation of antibacterial and antifungal activity

Using the agar well diffusion technique the final batch was tested for its antibacterial activity in contradiction of *S. aureus*, *B. subtilis*, *E. coli*, and *X. campestris* as well as its antifungal bustle in contradiction of *Aspergillus niger*. Azithromycin and clotrimazole were the most commonly utilized antibacterial and antifungal medications. The inhibitory zones diameters were measured.

## RESULT AND DISCUSSION

### Phytochemical Screening of Seeds and Leaves Extract

Utilizing reagent assays it was discovered that *A. squamosa* leaf extract contained several phytochemicals. Numerous primary and secondary metabolites with high biological relevance were found as a result of the phytochemical screening. In this work, a phytochemical examination of *A. squamosa* seed extract confirmed the presence of several phytochemicals, including alkaloids, carbohydrates, flavonoids, saponins, terpenoids, glycosides, steroids, and tannins. And phytochemical examination of *A. squamosa* leaf extract demonstrated the presence of phytoconstituents, including alkaloids, carbohydrates, flavonoids, saponins, glycosides, steroids, tannins, and proteins.

### Silver Nanoparticle Synthesis

The initial color of AgNO<sub>3</sub> was changed to dark brown with addition of extract of *A. squamosa* L. after reaction. These color changes in the reaction mixture powerfully specify the reduction of silver. Due to the development of Ag crystal in reaction mixture, pointed and thin peak emerge at 430 & 440 nm for AgNPs of *A. squamosa* L. seed and leaves correspondingly, as shown in Figure 2.

### Characterization of Developed Silver Nanoparticles

AgNPs developed by utilizing *A. squamosa* L seeds and leaves have been determined by following Characterization methods.

#### UV-vis Spectroscopy Studies

*A. squamosa* L prepared AgNPs scanned in 300 to 800 nm wavelength range using UV-visible spectrophotometer (Double beam, Shimadzu, UV- 800) to prove the formation of AgNPs.

##### • UV Spectra of AgNPs of *A. squamosa* L. seeds

Due to the AgNPs' "SPR," AgNPs generated in the process after 20 minutes had an absorption maximum at 430 nm. Silver nitrate's transformation into silver nanoparticles is due to 20 metabolites contained in the seed extract, such as polyphenols and fatty acids. The peak's expansion indicated the development of polydisperse nanoparticles as well.

##### • UV spectra of AgNPs of *A. squamosa* L. leaves

AgNPs molded in the reaction mix's absorption bands. Flavonoids may play a key function in the reduction progression for the bioformation of AgNPs after 20 min from the start of the reaction have an absorption maximum at 440 nm. As a result, the high concentration of flavonoids and phenolic acids in *A. squamosa*'s aqueous leaf extract examines the possibility of silver nitrate being bio-reduced to silver nanoparticles. The peak's expansion also showed that polydisperse nanoparticles had formed.

#### XRD

The microstructures of the produced AgNPs of *A. squamosa* L. form and the origin of the NP's as supported by the XRD. The Division of Physics at Uni. Shivaji Kop performed the laboratory tests as a result of XRD.

##### • XRD of Silver Nanoparticles of *A. squamosa* L. seed

The biosynthesized seeds AgNPs' XRD pattern revealed two strong peaks with 2 values ranging from 10 to 90. JCPDS has released XRD spectra of pure crystalline silver formations (File no.04-0783). The crystalline phase of the Ag atoms produced was established by an appraisal of the XRD band along with reference. It is possible to index the peaks at 2 values 33.55° and 39.63° as (111), and (200), respectively, of face-centered cubic planes of Ag. The (111) sets planes of lattice whose Bragg reflections may be indexed using the cubic face-centered construction of Ag were observed. Thus, it was evident from the XRD pattern that the Ag nanoparticles were crystal clear.

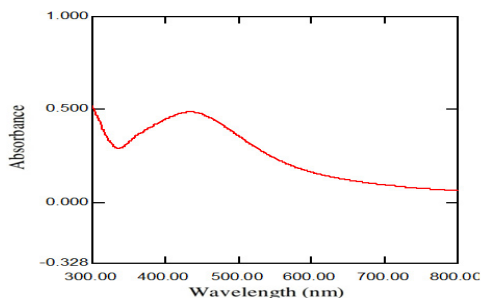


Figure 2: UV spectra of AgNPs of *A. squamosa* L. seeds

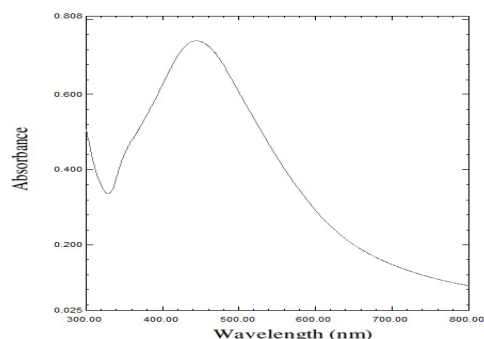


Figure 3: UV spectra of silver nanoparticle of *A. squamosa* L. leaves

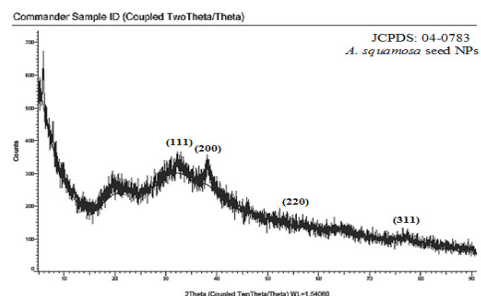


Figure 4: XRD of silver nanoparticle of *A. squamosa* L. seed

##### • XRD of Silver Nanoparticles of *A. squamosa* L. leaves

The biosynthesized leaves AgNPs' XRD pattern revealed three distinct peaks with 2 values ranging from 10 to 90. The JCPDS has released XRD spectra of pure crystalline silver formations (File no.04-0783). The crystalline phase of the silver particles produced in our research was established by assessment of the XRD band with reference. The three face-centered cubic silver planes at 2 values 27.75°, 33.55°, and 46.15°, 77.6° can be indexed as (110), (111), (211), and (311) correspondingly. The (111) sets of planes lattice whose Bragg reflections may be represented using the face-centered cubic construction of Ag were observed. Thus, it was evident from the XRD pattern that the Ag nanoparticles were crystal clear.

#### Particle-size

Crystallite size analysis is used to quantify the Ag nanoparticles of *A. squamosa* L. that range in diameter from 1 to 1000 nm depending on the application. The physics division at the A.S.D.C. of Pharmacy in Ashta conducted the samples for the nanometer dimensions.

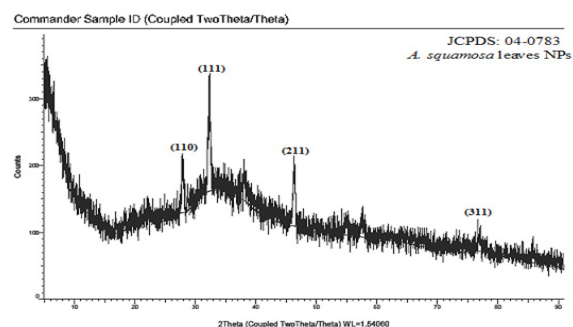


Figure 5: XRD of silver nanoparticle of *A. squamosa* L. leaves

The results obtained from silver nanoparticles are shown in Tables 2 to 4 and Figures 6 and 7

**Table 2:** Particle size and PI of metallic nanoparticles

Metallic nanoparticles	Particle size (in nm)	Polydispersity Index (PI)
Silver nanoparticle ( <i>squamosa</i> L. seed)	73.5	0.036
Silver nanoparticle ( <i>squamosa</i> L. leaves)	84.9	0.367

Particle size of Silver Nanoparticles of *A. squamosa* L. seeds

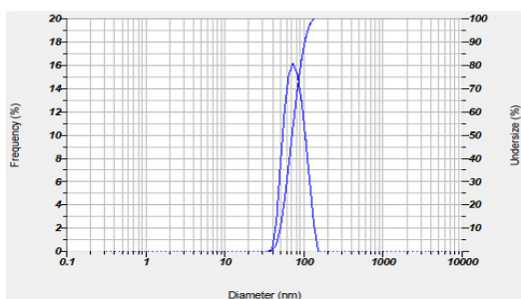


**Figure 6:** Particle size spectra of silver nanoparticles of *A. squamosa* L. seeds

**Table 3:** Particle size ranges of AgNPs of *A. squamosa* seeds

Peaks	S.P.R.	Mean (nm)	S. D. (nm)	Mode (nm)
1	1.00	73.5	18.8	67.6
2	---	---	---	---
3	---	---	---	---
Overall	1.00	73.5	18.8	67.6

Particle size of Silver Nanoparticles of *A. squamosa* L. leaves

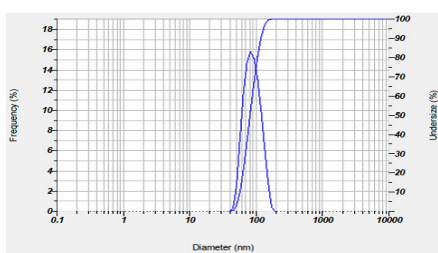


**Figure 7:** Particle size spectra of silver nanoparticle of *A. squamosa* L. leaves

**Table 4:** Particle size ranges of AgNPs of *A. squamosa* leaves

Peaks	S.P.R.	Mean(nm)	S. D.(nm)	Mode(nm)
1	1.00	84.9	33.5	77.9
2	---	---	---	---
3	---	---	---	---
Overall	1.00	84.9	33.5	77.9

**Scanning-electron-microscopy (SEM)**

Perusing of SEM were hackneyed to engender imagery of the developed metallic NPs of *A. squamosa* L. by scrutinize of exterior part with inattentive ray of the electrons. The SEM investigation be conceded at CFC of Uni. Shivaji. Kop

Characterization of SEM studies of *A. squamosa* seeds AgNPs

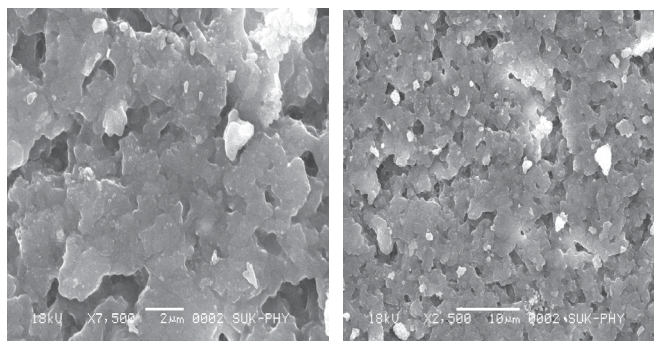


**Figure 8:** SEM image of *A. squamosa* seeds AgNPs

Characterization of SEM studies of *A. squamosa* leaves AgNPs

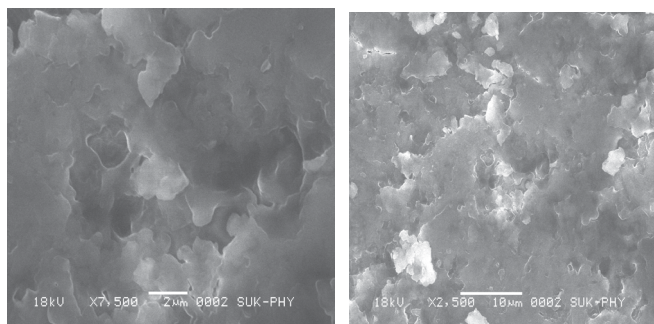


**Figure 9:** SEM image of *A. squamosa* leaves AgNPs

**Fourier Transform of Infrared Spectroscopy i.e., FTIR**

FTIR of Ag nanoparticles with use of *A. squamosa* L. (seeds and leaves). Was conceded at A.S.D.C. of pharmacy (Figures 10 and 11 and Tables 5 and 6).

FTIR of Silver nanoparticle of *A. squamosa* L. seeds

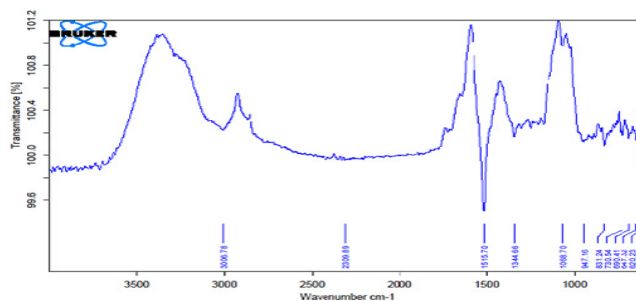


**Figure 10:** FTIR spectra of AgNPs of *A. squamosa* L. seeds

**Table 5:** FTIR result of AgNPs of *A. squamosa* L. seeds

Observed peak (cm <sup>-1</sup> )	Functional group present	Interpretation
620.23	Alkyne	C-H bend
690.41	Alkene	C=C stretch
831.24	Alkylhalide	C-Cl stretch
1068.70	1 <sup>0</sup> amine	CN stretch
1344.66	2 <sup>0</sup> amine	CN stretch
3006.78	Alkenes	=C-H stretch

FTIR of Silver nanoparticle of *A. squamosa* L. leaves

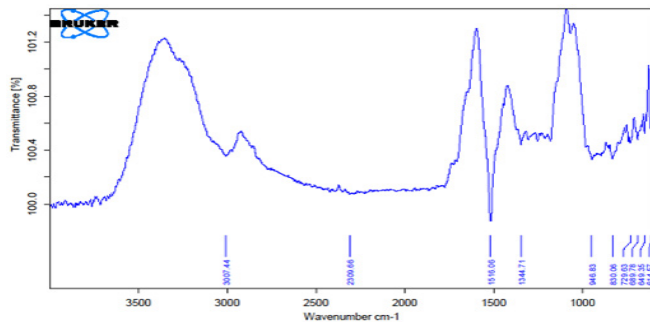


Figure 11: FTIR spectra of AgNPs of *A. squamosa* L. leaves

Table 6: FTIR result of AgNPs of *A. squamosa* L. leaves

Observed peak (cm <sup>-1</sup> )	Functional group present	Interpretation
614.57	Alkyne	C-H bend
729.63	Alkene	C=C stretch
830.06	1,4-distribution	C-H bend
946.83	Alkene	C-H bend
1516.06	Aromatic compound	C=C stretch
3007.44	Alkenes	=C-H stretch

Pharmacological Evaluation of Prepared AGNPs

Antibacterial activity

Measured in terms of inhibition area. Silver nanoparticles have various effects on the bacteria *E. coli*, *B. subtilis*, *X. campestris*, and *S. aureus*. Silver nanoparticles antibacterial activity has great results in contradiction of both gram ve<sup>+</sup> and gram ve<sup>-</sup> bacteria (Tables 7 and 9 and Figures 12 and 13).

Antibacterial activity of silver nanoparticle (*A. squamosa* L. seeds)

Table 7: Zone of the Inhibition of the AgNP's of *A. squamosa* L. seed

Sample	Zone of inhibition diameter (mm) against the selected microorganisms			
	<i>E. coli</i>	<i>B. subtilis</i>	<i>X. campestris</i>	<i>S. aureus</i>
AgNP's of <i>A. squamosa</i> L. seed	15	21	20	17
azithromycin (marketed drug)	20	25	25	21

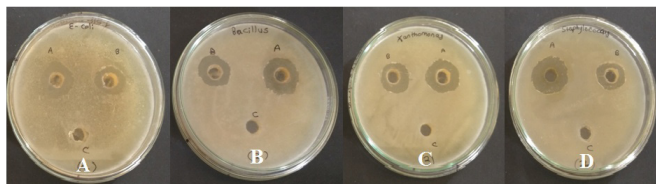


Figure 12: Antibacterial activity of AgNPs against (A) *E. coli*, (B) *B. subtilis*, (C) *X. campestris*, (D) *S. aureus*

The AgNPs of *A. squamosa* L. seeds show more zone of inhibition (21 mm) for *B. subtilis*.

Antibacterial activity of silver nanoparticle (*A. squamosa* L. leaves)

Table 8: Zone of the Inhibition of the AgNP's of *A. squamosa* L. leaves

Sample	Zone of inhibition diameter in mm versus selected microorganisms			
	<i>E. coli</i>	<i>B. subtilis</i>	<i>X. Campestris</i>	<i>S. Aureus</i>
Ag NP's of <i>A. squamosa</i> L. leaves	14	20	19	17
Azithromycin (marketed drug)	21	24	25	20

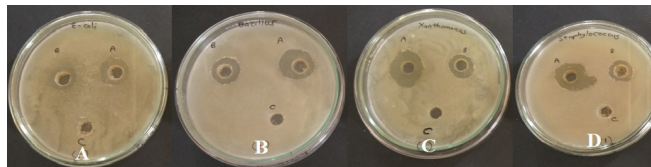


Figure 13: Antibacterial activity of Ag NPs against (A) *E. coli*, (B) *B. subtilis*, (C) *X. campestris*, (D) *S. aureus*

The AgNPs of *A. squamosa* L. leaves show more zones of inhibition (20 mm) for *Bacillus subtilis*.

Table 9: Zone of the Inhibition of the AgNPs of *A. squamosa* L. seed

No.	Sample	Zone of inhibition diameter in mm versus selected fungi
		<i>Aspergillus niger</i>
1.	Ag NP's of <i>A. squamosa</i> L. seeds	23
2.	clotrimazole (Marketed drug)	27

Antifungal activity

Relying on the interference area in millimeter, the fungus *A. niger* produces divergent results for the produced silver nanoparticles of *A. squamosa* L. seeds and leaves, referred to as samples A and B, appropriately (Table 10 and Figure 14).

Table 10: Zone of the Inhibition of the AgNPs of *A. squamosa* L. leaves

No.	Sample	Zone of inhibition diameter in mm versus selected fungi
		<i>Aspergillus niger</i>
1.	Ag NP's of <i>A. squamosa</i> L. leaves	22
2.	clotrimazole (Marketed drug)	28



Figure 14: Antifungal activity of (A) seed (B) leaves AgNPs against *A. niger*

Among both AgNPs of *A. squamosa* L. seeds and leaves the seeds AgNPs illustrates more antibacterial plus antifungal

action so the green synthesized AgNPs of *A. squamosa* L. seeds were additionally used for synthesis for topical gel formulation.

### Antioxidant Activity of Developed Nanoparticles

Bacterial, viral or parasitic infections trigger the creation of 'ROS' and 'RNS' which causes the oxidative stress so to reduce this oxidative stress the AgNPs are checked for the antioxidant activity along with antimicrobial activity.

AgNPs of *A. squamosa* L. seeds and leaves were tested for antioxidant activity using DPPH method and equated with customary drug ascorbic acid which possess IC<sub>50</sub> value 3.39 µg/mL which is already reported. The %inhibition and IC<sub>50</sub> value of DPPH uptake on AgNPs of *A. squamosa* L. seeds and leaves are seen in (Table 11)

**Table 11:** Antioxidant activity of AgNPs of *A. squamosa* L. seeds

Sample	Conc (µg/mL)	%inhibition	IC <sub>50</sub> (µg/mL)
AgNPs of <i>A. squamosa</i> L. seeds	10.0	57.70	18.95
	20.0	61.80	
	30.0	65.90	
	40.0	70.90	

**Table 12:** Antioxidant activity of AgNPs of *A. squamosa* L. leaves

Sample	Conc (µg/mL)	%inhibition	IC <sub>50</sub> (µg/mL)
AgNPs of <i>A. squamosa</i> L. leaves	10.0	51.30	21.35
	20.0	56.40	
	30.0	61.70	
	40.0	68.30	

The composites which possess IC<sub>50</sub> values ranging below 50 µg/mL is reflected to exhibit Very strong antioxidant bustle, the composites with IC<sub>50</sub> assessment oscillating between 50 to 100 µg/mL is considered to possess Powerful anti-oxidant activity, the compounds with IC<sub>50</sub> 100 to 50 µg/mL is considered to possess moderate anti-oxidant activity meanwhile the amalgams with IC<sub>50</sub> more than 150 µg/mL is considered to possess weak antioxidant activity (Table 12 ). In this case, both AgNPs of *A. squamosa* L. seeds and leaves possessed very strong antioxidant activity with IC<sub>50</sub> values 18.95 and 21.35 µg/mL (Table 13).

**Table 13:** Standard range of antioxidant activity

IC <sub>50</sub> (µg/mL)	Antioxidant activity
<50	Verystrongly
50–100	Powerful
100–150	Moderately
>150	Weakly

### In-vitro Anti-inflammatory Activity

There is a necessity to reduce inflammation caused due to microbial infection, so there is need to determine whether the generated AgNPs exhibit effective anti-inflammatory action or not.

### Inhibition Af albumin Aenaturation

In *in-vitro* anti-inflammatory activity by egg albumin denaturation method at a concentration of 100, 200, 300,

400 and 500 µg/mL exhibited 67.04, 69.34, 71.88, 74.28 and 75.31% inhibition of egg albumin denaturation for synthesized AgNPs of *A. squamosa* L. seeds (Table 14) and 61.28, 62.89, 65.09, 67.09 and 69.55% inhibition of egg albumin denaturation for synthesized AgNPs of *A. squamosa* L. leaves (Table 15) whereas, standard indomethacin at 100, 200, 300, 400 and 500 µg./mL which exhibited 74.03, 75.31, 77, 79.43 and 81.66% inhibition of egg albumin denaturation (Table 16). From this experimental comparison between mockups and standard consequences indicated noteworthy inhibition of egg albumin denaturation reliant on concentration.

**Table 14:** *In-vitro* anti-inflammatory activity of AgNPs of *A. squamosa* L. seeds

Treatment	Conc (µg/mL)	abs	%inhibition
AgNPs of <i>A. squamosa</i> L. seeds	100	0.1287	67.04
	200	0.1197	69.34
	300	0.1098	71.88
	400	0.1004	74.28
	500	0.0964	75.31

**Table 15:** *In-vitro* anti-inflammatory activity of AgNPs of *A. squamosa* L. leaves

Treatment	Conc (µg/mL)	abs	%inhibition
AgNPs of <i>A. squamosa</i> L. leaves	100	0.1512	61.28
	200	0.1449	62.89
	300	0.1363	65.09
	400	0.1285	67.09
	500	0.1189	69.55

**Table 16:** *In-vitro* anti-inflammatory activity of indomethacin

Treatment	Conc (µg/mL)	abs	%inhibition
Indomethacin	100	0.1014	74.03
	200	0.0964	75.31
	300	0.0898	77.00
	400	0.0803	79.43
	500	0.0716	81.66

### Preparation of Formulation

While from above data originate AgNPs formulated by utilizing *A. squamosa* L. seeds extract include enhanced activity than AgNPs prepared by using *A. squamosa* L. leaves extract so we used it for the preparation of formulations. Carbopol 940, chitosan and HPMC were used as gelling agents in formulations. Gels were formulated by cold mechanical technique.

### Evaluation Tests of Formulation

#### *Determination of clarity, color and odor*

The clarity and color are checked visually. Some of the batches are turbid while some batches are translucent in nature. The color of gel varies depending on the gelling agent. The odor is unwavering through stinking sense.

**Table 17:** Clarity and color of prepared batches of gel

Formulation	Clarity	Color	Odor
AF1	Translucent	Milky white	Characteristic
AF2	Translucent	Milky white	Light
AF3	Translucent	Milky white	Very light
AF4	Turbid	Green	Characteristic
AF5	Turbid	Green	Characteristic
AF6	Turbid	Green	Light
AF7	Translucent	White	Characteristic
AF8	Translucent	White	Light
AF9	Translucent	White	Very light

*pH*

Since the pH of humanoid skin is between 5.4–5.9, all developed gel batches illustrate pH assortment between 6.3–6.95, which are regarded fitting to evade the danger of exasperation when smeared to the skin (Table 18).

**Table 18:** pH of prepared batches

Batches	pH
AF1	6.3 ± 0.2
AF2	6.5 ± 0.2
AF3	6.8 ± 0.2
AF4	6.4 ± 0.2
AF5	6.95 ± 0.2
AF6	6.8 ± 0.2
AF7	6.4 ± 0.2
AF8	6.7 ± 0.2
AF9	6.4 ± 0.2
Silverx gel	7.1 ± 0.2

*Viscosity*

Using a Brookfield viscometer, the prepared gel’s viscosity was measured (Model RVTDV II). The formulation batch AF3, AF6, and AF9 had the highest viscosity of any of these formulations. out of this AF6 batch displays results that are close to the manufactured gel (Table 19).

**Table 19:** Viscosity of prepared batches

Batches	Viscosity (cp)
AF1	2400
AF2	2560
AF3	2884
AF4	2638
AF5	2889
AF6	3020
AF7	2498
AF8	2981
AF9	3025
Silverx gel	3037

*Spreadability*

The spreadability in circles had sizes ranging from 34 to 48 mm. Chitosan gel has the lowest spreadability, whereas Carbopol gel has the most spreadability. The findings showcase that as gelling agent concentration was raised, the gel’s spreadability reduced, as seen by the smaller width of the spread circle (Table 20).

**Table 20:** Spreadability of prepared batches

Batches	Spreadability (cm <sup>2</sup> /gm)
AF1	0.320
AF2	0.270
AF3	0.250
AF4	0.280
AF5	0.250
AF6	0.230
AF7	0.290
AF8	0.270
AF9	0.260
Silverx gel	0.220

*Extrudability*

During solicitations and patient acceptance, the tube’s gel extrusion is crucial. In order to push the gel out of the tube, an appropriate consistency is needed. Gels with elevated constancy may not do so, but low viscous gels may flow easily (Table 21).

**Table 21:** Extrudability of AgNP’s gel

Formulation	Formulation weight (gm)	Gel extruded weight (gm)	Extrud	Appear
F1	15.15	13.22	87.26	++
F2	15.30	12.98	84.83	++
F3	15.43	11.91	77.18	++
F4	14.95	12.80	85.61	++
F5	15.34	13.90	90.61	+++
F6	15.40	11.86	77.01	++
F7	14.88	13.02	87.05	++
F8	15.30	13.81	90.26	+++
F9	15.41	11.99	77.80	++
Silverx gel	17.50	16.05	91.71	+++

Note: + fair, ++ good, +++ excellent

*Centrifugation test*

Total of 10 g of the formulation were put to a centrifugation tube to demeanor the centrifugation assessment. The sample gel underwent centrifugation and was spun at 2000 rpm for half hour at room temperature.

Formulations were kept under steady conditions throughout the experiments. There was not any phase separation observed during the centrifugation/spinning test.

### Optimization of batch

After checking different evolution parameters like pH, viscosity, extrudability & spreadability of AF1 to AF9 batches of gel we found that AF3, AF6 & AF9 batches show good results as compared to the other batches of gel so we select AF3, AF6 & AF9 batches for *in-vitro* diffusion studies (Table 22).

### Drug Release Data

#### *In-vitro* diffusion studies

Table 23 shows the *in-vitro* propagation contour of the AF3, AF6, and AF9 preparations. The phosphate buffer saline (7.4 pH) was employed for the *in-vitro* scientific data of the gel phases since the pH of the film used was in the range of 5 to 7.8. The *in-vitro* release profiles were carried out for 6 hours for each of the prepared compounds (Table 23).

**Table 22 :** Calibration table

Sr. No.	Concentration	Absorbance (at 455 nm)
1	2	0.279
2	4	0.468
3	6	0.646
4	8	0.764
5	10	0.881

**Table 23:** Percent drug release of AF6, AF3, AF9 batch

Time	%drug release of AF6	%drug release of AF3	%drug release of AF9
0	0	0	0
30	0.623	0.7480	0.7480
60	1.589	1.8381	1.683
90	2.7731	2.838	2.7428
120	4.643	4.833	4.706
150	7.199	7.3870	6.950
180	10.254	10.254	9.506
210	15.895	15.17	12.3116
240	25.277	23.906	16.114
270	37.028	34.722	22.628
300	49.869	47.033	33.288
330	64.830	61.901	45.225
360	81.386	77.236	60.476

### Determination - Antibacterial & Antifungal Activity of gel

We only chose batch AF6 for antibacterial and antifungal activities because we discovered that it produces results that are suitable for it to become an optimal gel. In this investigation,

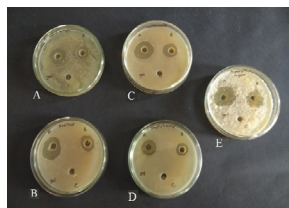


**Figure 15:** Antibacterial, antifungal activity of Ag NPs *A. squamosa* L. against (A) *E. coli*, (B) *B. subtilis*, (C) *X. campestris*, (D) *S. aureus*, (E) *A. niger*

**Table 24:** Zone of the Inhibition of formulated gel using synthesized AgNPs *A. squamosa* L. seeds

Sr. No.	Sample	Zone of inhibition diameter in mm versus selected microorganisms				
		<i>E. coli</i>	<i>B. subtilis</i>	<i>X. campestris</i>	<i>S. aureus</i>	<i>A. niger</i>
1.	Batch F5	13	19	18	16	18
2.	Silverex gel (matket.)	19	23	22 mm	20	--
3.	KANSEL-DS gel (matket.)	--	--	--	--	25

regular Silverex gel and Kinsel-DS gel were cast off to investigate the antibacterial and antifungal activities (Figure 15 and Table 24).

### CONCLUSION

AgNPs were fashioned using the green synthesis tactic by extracting the seeds and leaves of *A. squamosa* L. as a reducing mediator. Once the reaction is comprehensive, the tint of the NPs changes from colorless to milky white for seeds and dark brown for leaves. UV-vis spectroscopy also sanctions the amalgamation of AgNPs since it exhibits divergent peaks at 430 and 440 nm for synthesized AgNPs of seeds and leaves, respectively. The face-center-cubic structure of the Ag crystal is visible in the XRD profile, and the crystallites were established mostly in the plane. For synthesized AgNPs, the fourier transform of infrared spectroscopy analysis and SEM was effectively explored. Pharmacological investigations' findings advocate that synthetic AgNPs made from *A. squamosa* L. seeds extract have superior antibacterial, antioxidant, and anti-inflammatory properties as compared to AgNPs made from leaf extract. Finally, several features of gel formulations containing silver nanoparticles were evacuated. The characterization of the gel had revealed that the formulation's pH was moving closer to neutrality. The AF6 batch's viscosity, spreadability, and extrudability were much closer to the commercial product's.

### REFERENCES

1. Khan I, Saeed K, Khan I. Nanoparticles: properties, applications and toxicities, Arab J Chem.2019;12 (7): 908-931. <https://doi.org/10.1016/j.arabjc.2017.05.011>
2. Mansoori GA, Soelaiman TAF. Nanotechnology – an introduction for the standards community. Journal of ASTM International.2005;2(6) :1-22. Paper ID JAI13110
3. Sunil K. Sharma, Azhar U. Khan, Masudulla Khan et al. Biosynthesis of MgO nanoparticles using *A squamosa* seeds and its catalytic activity and antibacterial screening. Micro & Nano Letters.2020;15(1):30–34.
4. Vimala Jose, Lidiya Raphel, K. S. Aiswariya, Paulson Mathew. Green synthesis of silver nanoparticles using *A squamosa* L. seed extract: characterization, photocatalytic and biological activity assay, Bioprocess and Biosystems Engineering.2016. <https://doi.org/10.1007/s00449-021-02562-2>
5. Kalyani et al. Synergetic Antibacterial Effect of Biosynthesized Silver Nanoparticles, Indian J Pharm Sci. 2019; 81( 6):1036-1044.

6. K. Velsankar, Aswin Kumar R.M., Preethi R., Muthulakshmi V., S. Sudhahar. Green synthesis of CuO nanoparticles via *Allium sativum* extract and its characterizations on antimicrobial, antioxidant, antilarvicidal activities, *Journal of Environmental Chemical Engineering*. 2020;8(5):104-123.
7. Prabhu N., Divya T.R., Yamuna G. Synthesis of silver phytonanoparticles and their antibacterial efficacy. *Dihest. J Nanomater Biostruct*.2010;Vol. 5:185-189.
8. Singh A, Jain D, Upadhyay MK, Khandelwal N, Verma HN. Green synthesis of silver nanoparticles using *Argemone mexicana* leaf extract and evaluation of their antimicrobial activities. *Dige J Nanomater and Biostruc*. 2010; 5(2):483-489.
9. Swapna Suresh Joshi, A. K. Sahoo, Neeraj R. Prasad and Iranna S. Udachan. biosynthesis of silver nanoparticles (AgNPs) by extract of *A squamosa* waste: characterization and their antimicrobial activity, *International Journal of Research and Analytical Reviews*. 2018;5( 4): 907-914.
10. Pooja singh, Kshitij RB Singh, Jay Singh, Subha Narayan Das and Ravindra Pratap Singh. Tunable electrochemistry and efficient antibacterial activity of plant-mediated copper oxide nanoparticles synthesized by *A squamosa* seed extract for agricultural utility. *RSCAdv*.2021. DOI:10.1039/d1ra02382a
11. Chengyao Ma et al. A Review on *A squamosa* L.: Phytochemicals and Biological Activities, *The American Journal of Chinese Medicine*.2017; 45(5):1–32.
12. Lin, C. S. K., Pfaltzgraff, L. A., Herrero-Davila, L., Mubofu, E. B., Abderrahim, S., Clark, J. H., and Thankappan, S. Food waste as a valuable resource for the production of chemicals, materials and fuels. *Current situation and global perspective, Energy and Environmental Science*. 2013;6 (2): 426-464.
13. Korkmaz N, Ceylan Y, Taslimi P, Karadag A, Bulbul AS, Sen F. Biogenic nano silver: synthesis, characterization, antibacterial, antibiofilms, and enzymatic activity, *Adv Powder Technol*.2020; Vol. 31:2942–2950.
14. S. Sukumar, A. Rudrasenan and D. Padmanabhan Nambiar. Green-Synthesized Rice-Shaped Copper Oxide Nanoparticles Using *Caesalpinia bonducella* Seed Extract and Their Applications, *ACS Omega*.2020;Vol. 5: 1040–1051.
15. Calderón-Jiménez, Bryan; Johnson, Monique E.; Montoro Bustos, Antonio R.; Murphy, Karen E.; Winchester, Michael R.; Vega Baudrit, José R. *Silver Nanoparticles: Technological Advances, Societal Impacts, and Metrological Challenges*, *Frontiers in Chemistry*. 2017. doi:10.3389/fchem.2017.00006
16. Roe, D.; Karandikar, B.; Bonn-Savage, N.; Gibbins, B.; Rouillet, J.-B. Antimicrobial surface functionalization of plastic catheters by silver nanoparticles. *J. Antimicrob. Chemother*. 2008;Vol. 61: 869–876.
17. Qing, Y.; Cheng, L.; Li, R.; Liu, G.; Zhang, Y.; Tang, X.; Wang, J.; Liu, H.; Qin, Y. Potential antibacterial mechanism of silver nanoparticles and the optimization of orthopedic implants by advanced modification technologies. *Int. J. Nanomed*.2018;5(13): 3311-3327. doi: 10.2147/IJN.S165125
18. Seong, M.; Lee, D.G. Silver nanoparticles against *Salmonella enterica* serotype typhimurium: Role of inner membrane dysfunction, *Curr. Microbiol*.2017;74(6)661-670. doi: 10.1007/s00284-017-1235-9
19. Kailasa, S.K.; Park, T.-J.; Rohit, J.V.; Koduru, J.R. Antimicrobial activity of silver nanoparticles. In *Nanoparticles in Pharmacotherapy*; Elsevier: Amsterdam, The Netherlands. 2019;461–484.
20. Rijuta Ganesh Saratale. New insights on the green synthesis of metallic nanoparticles using plant and waste biomaterials: current knowledge, their agricultural and environmental applications. *Environmental Sciences and Pollutant Research*.2017. DOI 10.1007/s11356-017-9912-6
21. Mohsin J. Jamadar, Rajmahammad Husen Shaikh. preparation and evaluation of herbal gel formulation, *Journal of Pharmaceutical Research & Education*. 2017;Vol. 1( 2): 201-224.
22. Kavitha. K, Kavitha. T, Reshma Fathima. K preparation and evaluation of herbal gel formulation of *cissus vitiginea* leaf, *Journal of Pharma Research*. 2018;7 (7): 179-181.
23. Amiya Kumar Prusty and Prasanna Parida. Development and Evaluation of Gel Incorporated with Biogenically Synthesised Silver Nanoparticles, *Journal of Applied Biopharmaceutics and Pharmacokinetics*. 2015;Vol.3:1-6.
24. Singh M.K., Khare G., Iyer S., Sharma G., Tripathi D.K. *Clerodendrum serratum*: A Clinical approach, *JAPS*. 2012; 2 (2): 11-1.